Available online at www.eccomasproceedia.org
Eccomas Proceedia COMPDYN (2023) 1392-1399

ECCOMAS
Proceedia

COMPDYN 2023
9th ECCOMAS Thematic Conference on
Computational Methods in Structural Dynamics and Earthquake Engineering
M. Papadrakakis, M. Fragiadakis (eds.)
Athens, Greece, 12-14 June 2023

PREDICTION OF THE STATIC AND FATIGUE PERFORMANCE OF PITTED STEEL WIRE ROPES

Aldo Milone[1]

[1] Department of Structures for Engineering and Architecture
Via Forno Vecchio 36, 80134, Naples, Italy
e-mail: aldo.milone@unina.it

Abstract

Wire strands made of high-strength steel (HSS) are largely employed in bridge engineering for the realization of deck support systems (cable-stayed bridges). Owing to their peculiar destination of use, cable-stayed bridges are usually placed in aggressive environments. Hence, significant corrosion processes can occur in strands if not correctly protected, resulting in a substantial decrease of both their static and fatigue resistance. Non-uniform and localized corrosion (i.e., "pitting") can further worsen the performance of HSS wire strands. Thus, assessing the static and cyclic response of existing cables adopted for bridges is crucial for a proper estimation of the remaining service life of the entire structure. Within this context, in this work a model to predict the static and fatigue performance of pitted HSS strands is presented. Corroded parts of steel wires are modelled via spring elements accounting for the real pit geometry. An application of the Strain Energy Density (SED) method is presented to derive constitutive behavior of such elements. Predictions made with the described model are finally compared with experimental results on real corroded elements drawn from literature.

Keywords: Fatigue, Material Degradation, Wire Ropes, Pitting Corrosion

ISSN:2623-3347
Peer-review under responsibility of the organizing committee of COMPDYN 2023.
doi: 10.7712/120123.10484.20396

1 INTRODUCTION

When designing bridges to cross significant spans, staying cables arguably represent a competitive solution for carrying bridge deck and traffic loads [1]. Such cables undergo rather strong tensile actions during their service life due to the combined effect of static loads (i.e., bridge self-weight, weight of non structural components such as pavement and safety rails) and cyclic actions (i.e., traffic, wind, earthquakes). Therefore, a critical focus is needed in correctly assessing the structural behavior of such details. Indeed, as largely shown in scientific literature, detailing may play a decisive role in affecting the global response of steel and composite structures [2-24]. For instance, with reference to typical cable-stayed bridges, a local collapse of a single cable can lead to disproportionate bridge failure owing to the lack of structural redundancy.

Staying cables are usually manufactured using high-strength steels (HSS), namely in form of wire ropes made by arranging multiple layers of 7-wire strands [1]. Although a proper protective coating is always needed according to EN:1993-1-11 indications [25], the elevated aspect ratio of strands leaves them often exposed to surficial corrosion. Indeed, due to the typically long service life of existing cable-stayed bridges, such preventive measures (e.g., zinc coating) become gradually ineffective, hence exposing outer wires to aggressive exogenous agents.

This condition can result in strongly localized damage (pitting [1]), which impairs both the tensile and fatigue performance of HSS wires in dependence from several factors [1]. In light of this, assessing static and cyclic behavior of corroded steel ropes still represents an open and wide field of research. Within this framework, in the present work an analytical model to predict tensile and cyclic behavior of pitted HSS strands is presented, i.e., based on an application of the SED method [26-28].

The paper is mainly divided in two parts. In the first section, features of the proposed model are discussed. Finally, a first validation of the model is reported with tests drawn from literature.

2 MODEL FEATURES

The proposed model for corroded HSS wire ropes features a sub-assemblage of in which individual wires are assumed as base components (Figure 1). Corroded wires are modelled by means of three distinct, in-series axial springs. Namely, while the inner spring represents the damaged portion of the wire, outer ones account for its pristine ends. Intact wire parts are regarded as indefinitely elastic up to failure, while damaged portions behave elasto-plastically. Static and fatigue strength of damaged portions has been assessed by means of a FEM-based application of the SED method (Figure 2) [26-28].

FEM modelling of pitted wires was developed using ABAQUS v. 6.14 software [29]. C3D10 elements (10 node–tetrahedron, quadratic geometry, standard integration) were used to discretize each part. Wires symmetry was explicitly accounted for to balance computational effort with analyses accuracy. According to the SED method [26-28], static (fatigue) failure is governed by averaged strain energy density – ASED (range) W (ΔW) over a control volume centered at the pit tip and having radius R_0.

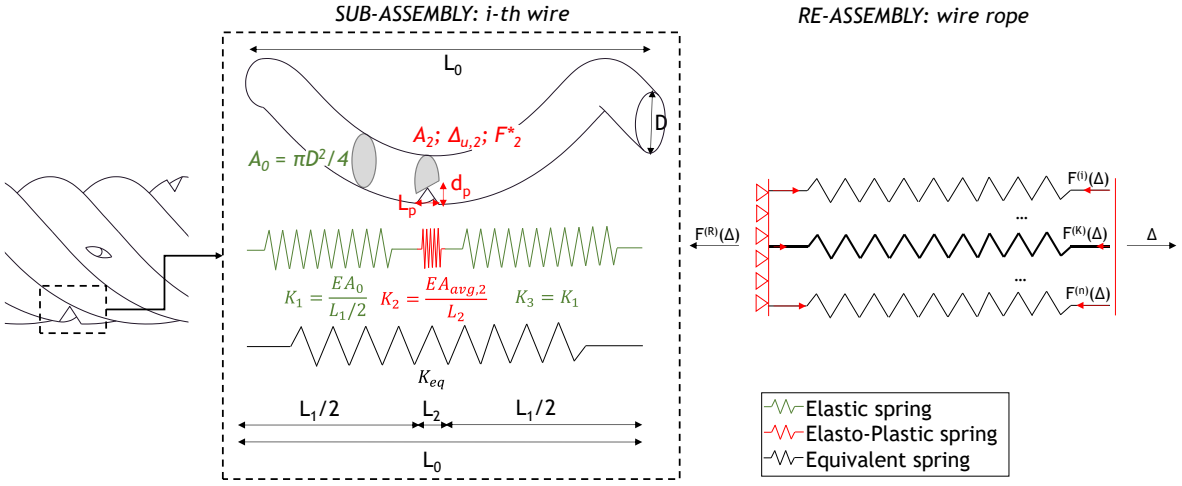

Figure 1: Equivalent modelling of a corroded wire rope.

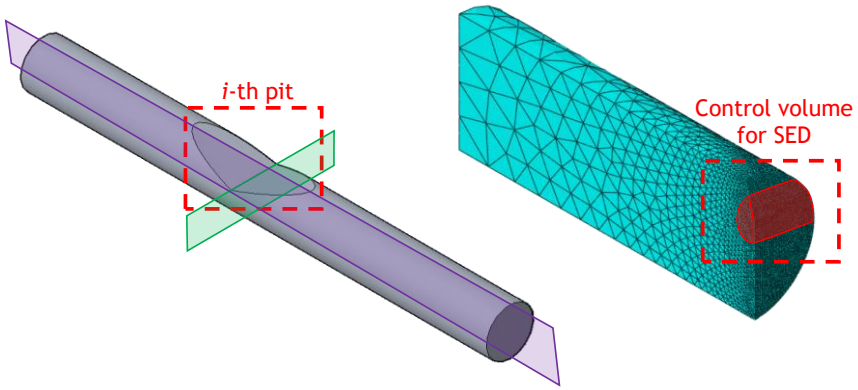

Figure 2: FEM-based application of the SED method for pitted wires.

Based on typical fracture toughness K_{IC} and ultimate tensile strength f_u for HSS [30], $R_0 = 0.28$ mm was assumed according to indications reported in [26-28].

2.1 Static behaviour of the proposed model

The proposed model behaves as a displacement-based system in static conditions, i.e. for monotonic tensile loads. Three subsequent behavior stages can be identified for the *i*-th wire, namely:

- Elastic – Under imposed displacements Δ smaller than Δ_e, the single wire model behaves as purely elastic, with Δ_e being the proportionality limit of the equivalent spring, i.e. the ratio among the wire peak resistance F*, which is calculated through the SED method [26-28], and the wire equivalent stiffness K_{eq} (Equation 1);

$$K_{eq} = \left(\frac{L_1 + L_3}{EA_0} + \frac{L_2}{EA_{min}}\right)^{-1} \tag{1}$$

- Plastic – Once the imposed displacements exceed the proportionality limit Δ_e, the single wire behaves as perfectly plastic. Namely, an axial plastic hinge forms in the damaged part; therefore, with F = F* being constant, the inner spring absorbs each new displacement increment, while the outer ones do not further elongate;
- Broken – Plastic stage lasts until the ultimate displacement of the wire Δ_u is reached. Subsequently, the *i*-th wire cannot sustain any further elongation increment and the explicated force drops to zero (that is, $F(\Delta > \Delta_u) = 0$).

The tensile behavior of the whole rope is derived by assuming a system of N wires in parallel (i.e., subjected to the same displacement $\Delta_1 = \Delta_2 = \ldots = \Delta$, Figure 3a).

Accordingly, the secant stiffness of the wire rope gradually reduces as more wires enter the plastic range. Hence, when the most brittle wire fails, the explicated force F_R abruptly decreases. However, collapse of the first wire does not always imply that the peak resistance of the rope has been reached. Indeed, less damaged wires can usually still sustain further elongations with an increase of the overall rope reaction. Finally, when the peak tensile resistance $F_{R,max}$ is attained, the rope quickly fails due to the sequential collapse of several wires, as they are cannot redistribute internal forces without breaking in turn. This phenomenon, which is usually referred as waterfall break in scientific literature, is a peculiarity of HSS wire ropes. Hence, the resulting behavior is quasi-brittle, as opposed to the usual ductility exhibited by steel structural details [2-24].

2.2 Fatigue behaviour of the proposed model

The proposed model behaves as a force-based system in cyclic conditions, i.e. for fatigue loads (Figure 3b). The applied fatigue load is distributed among wires in proportion to the ratio among their equivalent stiffness $K_{eq,i}$ and the secant stiffness of the rope K_R as follows (Equation 2):

$$\Delta\sigma_i = \frac{K_{eq,i}}{K_R}\frac{\Delta F_R}{A_{min,i}} = \frac{K_{eq,i}}{\sum_{i=1}^{N} K_{eq,i} - \sum_{i=1}^{B} K_{eq,i}}\frac{\Delta F_R}{A_{min,i}} \tag{2}$$

where B is the number of broken wires at a given step of fatigue analysis.

Fatigue strength of each wire is estimated through the SED method [26-28]. When the *i*-th wire breaks, the remaining $N - i + 1$ wires undergo a reduction of the fatigue strength owing to two simultaneous phenomena, i.e., *i*) the increment of applied stress range (see Equation 2) and *ii*) the presence of a prior damage deriving from previous cycles. The latter effect is accounted for by cumulating damage through the linear Palmgren-Miner model [1,4].

Fatigue analysis continues until the last wire reaches its residual fatigue strength. Hence, total fatigue life of the rope N_{fR} is calculated as the sum of fatigue life increments related to each wire ΔN_{fi}.

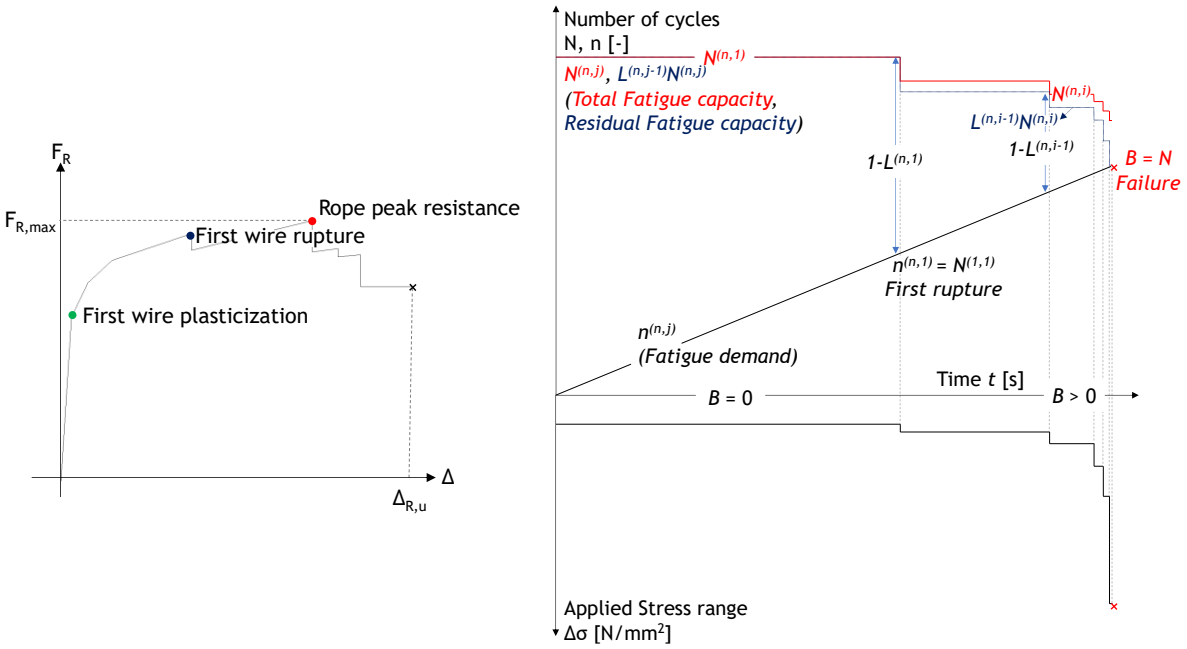

a) b)

Figure 3: a) Static and b) fatigue behavior of the proposed model.

2.3 Application of the SED method

Static strength of each wire has been calculated through FEM-based ASED calculations. Namely, according to [26-28], a weakened component fractures when the ASED in the control volume reaches the quantity $f_u^2/2E_s$. Based on performed finite element analyses, a resistance domain $F^*–d_p$ has been derived, with d_p being the pit depth (Figure 4a). Indeed, pit length L_p proved to have a minor influence on the static resistance of wires.

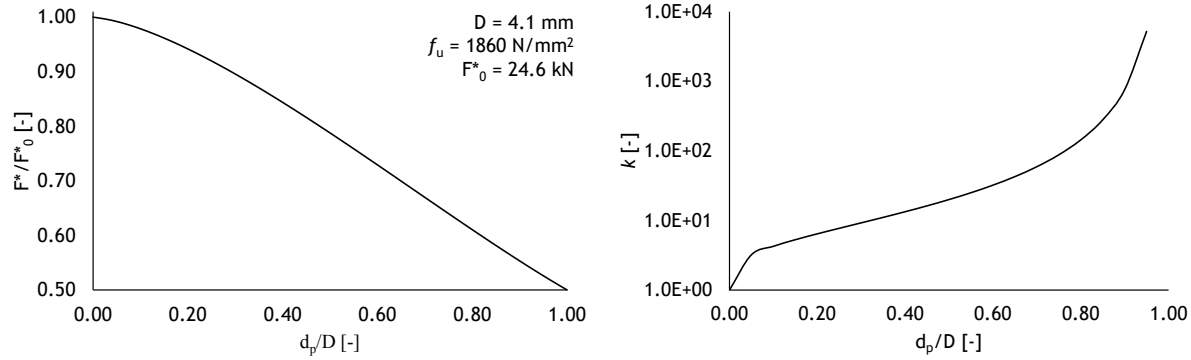

Figure 4: Performance domain of pitted wires: a) static and b) fatigue conditions.

As for fatigue conditions, equivalent, SED-based, stress magnification factors (*k*) for damaged parts have been derived, e.g., depending on pit geometry. Values of *k* are obtained by inverting the general

expression of ASED over a given control volume estimated for a unitary load (W_1) applied on the free end of the wire (Equation 3):

$$W_1 = W\left(\sigma_{gross} = 1\right) = \frac{(k \cdot 1)^2}{2E} \tag{3}$$

where W_1 is estimated through finite element analyses (Figure 4b).

It is worth remarking that such factors should be not intended as the ratio among nominally applied stress ranges on wire ends and "real" stress ranges acting at the pit tip. Indeed, *k* simply reduces applied stress ranges to equivalent stress ranges adopted for fatigue checks within the framework of the SED method.

3 APPLICATION TO CASE STUDIES

3.1 Validation for static conditions

A first validation of the proposed model in static conditions is thus illustrated as respect to experimental outcomes for real HSS corroded 7-wire strands employed as post-tensioning elements in dams anchor systems [31] (Figure 5).

Validation is carried out with reference to a wide set of 161 specimens with different degrees of corrosion η. Data for deepest pits and comparison against test results and predictions are summarized in Table 1 with reference to 9 representative specimens. Notably, the proposed model can reliably predict the tensile strength of corroded strands. The average predicted/experimental results ratio tensile is 1.02, with a low COV = 0.05. In light of these outcomes, the proposed model can be considered validated as respect to static conditions.

Table 1: Parameters and numerical predictions for representative corroded 7-wire strands [31].

Specimen Label [31] [-]	**η** [%]	**$d_{p,max}$** [mm]	**$L_{2,max}$** [mm]	**$F_{R,max}$** [kN]	**$F_{max,test}$** [kN]
8	7	0.6	2.4	256.3	253.6 (+2%)
38	14	0.7	2.8	239.6	233.1 (+2%)
73	25	1.2	10.1	221.4	204.2 (+7%)
99	34	1.7	7.6	186.3	179.8 (+3%)
112	43	1.7	6.9	153.9	155.2 (-2%)
133	55	1.7	17.1	127.2	122.0 (+4%)
143	67	3.1	10.2	94.9	89.3 (+6%)
156	78	3.7	20.4	60.4	58.6 (+3%)
160	83	3.9	15.7	45.2	45.0 (+0%)

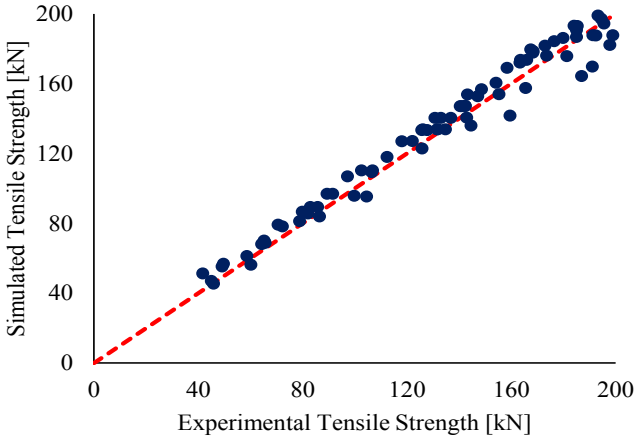

Figure 5: Validation of the model in static conditions.

3.2 Validation for fatigue conditions

The proposed model is hence validated in fatigue with respect to fatigue tests on pitted wires extracted from 7-wire HSS strands [32].

Validation is carried out with reference to a wide set of 61 specimens with different degrees of corrosion η. Pits geometry for tested wires is summarized in Table 2. Fatigue assessment of pitted wires according to the proposed, SED-based formulation, is summarized in Figure 6 (Wohler diagram). Notably, a rather high prediction accuracy is attained, as fatigue data are located within a very narrow scatter band (coefficient of determination $R^2 = 0.95$, scatter ratio $T_\sigma = 1.33$). In light of these outcomes, the proposed model can be considered validated as respect to fatigue conditions.

Table 2: Parameters for fatigue tests on pitted wires [32].

	Δσ [N/mm²]	**R [%]**	**d_p [mm]**	**L_2 [mm]**
MIN	270	0.4	0.18	0.36
MAX	840	0.5	0.68	9.93

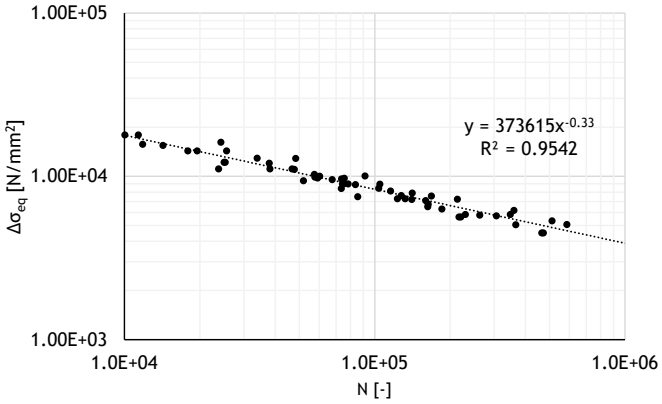

Figure 6: Validation of the model in fatigue conditions.

4 CONCLUSIONS

In the present work, a mechanical model for the prediction of the structural behavior of corroded wire ropes was presented and validated in this work against literature results. In light of reported outcomes, the following conclusions can be drawn:

- The proposed model is based on a sub-assembly of corroded ropes by means of elasto-plastic springs;
- In spite of its simplicity, the model predicted tensile resistance of corroded ropes tested in [31] with high accuracy;
- The fatigue resistance of pitted wires tested in [32] was also successfully predicted;
- Further studies are needed to further prove the reliability of the proposed formulation.

REFERENCES

[1] A. Milone, R. Landolfo, F. Berto, Methodologies for the fatigue assessment of corroded wire ropes: A state-of-the-art review. *Structures*, **37**, 787-794, 2022.

[2] A. Milone, M. D'Aniello, R. Landolfo, Influence of camming imperfections on the resistance of lap shear riveted connections. *Journal of Constructional Steel Research*, **203**, 107833, 2023.

[3] R. Tartaglia, A. Milone, M. D'Aniello, R. Landolfo, Retrofit of non-code conforming moment resisting beam-to-column joints: A case study. *Journal of Constructional Steel Research*, **189**, 107095, 2022.
[4] A. Milone, R. Landolfo, A Simplified Approach for the Corrosion Fatigue Assessment of Steel Structures in Aggressive Environments. *Materials*, **15**(6), 2210, 2022.
[5] R. Tartaglia, A. Milone, A. Prota, R. Landolfo, Seismic Retrofitting of Existing Industrial Steel Buildings: A Case-Study, *Materials*, **15**(9), 3276, 2022.
[6] G. Di Lorenzo, R. Tartaglia, A. Prota, R. Landolfo, Design procedure for orthogonal steel exoskeleton structures for seismic strengthening. *Eng. Struct.* 275, 115252, 2023.
[7] R. Tartaglia, M. D'Aniello, R. Landolfo, Seismic performance of Eurocode-compliant ductile steel MRFs, Earthquake Engineering and Structural Dynamics, 51(11), 2527-2552, 2022.
[8] R. Tartaglia, M. D'Aniello, F. Wald, Behaviour of seismically damaged extended stiffened end-plate joints at elevated temperature. *Engineering Structures,* **24**, 113193, 2021.
[9] R. Tartaglia, M. D'Aniello, R. Landolfo, Numerical simulations to predict the seismic performance of a 2-story steel moment-resisting frame, *Materials.* **13(21)**, 1-17, 2020.
[10] R. Tartaglia, M. D'Aniello, Influence of Transvserse Beams On the Ultimate Behaviour of Seismic Resistant Parrtial Strength Beam-To-Columnn Joints. *Ingegneria sismica*, **37(3)**, 50-65, 2020.
[11] M. D'Aniello, R. Tartaglia, S. Costanzo, G. Campanella, R. Landolfo, A. De Martino, Experimental tests on extended stiffened end-plate joints within equal joints project. *Key Engineering Materials*, **763**, 406 – 413, 2018.
[12] R. Tartaglia, M. D'Aniello, R. Landolfo, FREEDAM connections: advanced finite element modelling, Ingegneria sismica, **39**(2), 24-38, 2022.
[13] R. Tartaglia, M. D'Aniello, R. Landolfo, G.A. Rassati, J. Swanson, Finite element analyses on seismic response of partial strength extended stiffened joints, *COMPDYN 2017* - 4952-4964, 2017. 10.7712/120117.5775.17542.
[14] L. Fiorino, S. Shakeel, A. Campiche, R. Landolfo, In-plane seismic behaviour of lightweight steel drywall façades through quasi-static reversed cyclic tests, *Thin-Walled Structures*, **182**, 110157 2023.
[15] R. Landolfo, A. Campiche, O. Iuorio, L. Fiorino, Seismic performance evaluation of CFS strap-braced buildings through experimental tests, *Structures*, **33**, 3040-3054, 2021.
[16] A. Campiche, S. Costanzo, Evolution of EC8 seismic design rules for X concentric bracings, Symmetry, **12**, 1-16, 2020.
[17] Shakeel, S., Landolfo, R., Fiorino, L. Behaviour factor evaluation of CFS shear walls with gypsum board sheathing according to FEMA P695 for Eurocodes. *Thin-Walled Structures*. **141**, 194-207, 2019. https://doi.org/10.1016/j.tws.2019.04.017
[18] L. Fiorino, B. Bucciero, R. Landolfo, Shake table tests of three storey cold-formed steel structures with strap-braced walls. *Bulletin of Earthquake Engineering*, **17**(7), 4217-4245, 2019. https://doi.org/10.1007/s10518-019-00642-z.
[19] M. Pongiglione, C. Calderini, M. D'Aniello, R. Landolfo, NOVEL REVERSIBLE SEISMIC-RESISTANT JOINT FOR SUSTAINABLE AND DECONSTRUCTABLE STEEL STRUCTURES, Journal of Building Engineering, **35**, 101989, 2021, https://doi.org/10.1016/j.jobe.2020.101989
[20] M. Latour, M. D'Aniello, R. Landolfo, G. Rizzano, Experimental and numerical study of double-skin aluminium foam sandwich panels in bending. Thin-Walled Structures, **164**, 107894, 2021. DOI: 10.1016/j.tws.2021.107894

[21] M. Bosco, M. D'Aniello, R. Landolfo, C. Pannitteri, P-P. Rossi, Overstrength and deformation capacity of steel members with cold-formed hollow cross-section. *Journal of Constructional Steel Research*, **191**, 107187, 2022.https://doi.org/10.1016/j.jcsr.2022.107187
[22] A. Poursadrollah, M. D'Aniello, R. Landolfo, Experimental and numerical tests of cold-formed square and rectangular hollow columns. *Engineering Structures*, **273**, 115095, 2022. https://doi.org/10.1016/j.engstruct.2022.115095
[23] M. Latour, G. Rizzano, Seismic behavior of cross-laminated timber panel buildings equipped with traditional and innovative connectors Archives of Civil and Mechanical Engineering, **17(2)**, 382 – 399, 2017.
[24] M. D'Antimo, M. Latour, G.F. Cavallaro, J.-P. Jaspart, S. Ramhormozian, J.-F. Demonceau, Short- and long- term loss of preloading in slotted bolted connections. *Journal of Constructional Steel Research*, **167**, 105956, 2020.
[25] CEN. EN1993:1-11 - Eurocode 3 – Design of steel structures, Part 1-11: Design of structures with tension components, 2006, CEN, Brussel.
[26] F. Berto, P. Lazzarin, Recent developments in brittle and quasi-brittle failure assessment of engineering materials by means of local approaches, *Materials Science and Engineering R: Reports*, **75**(1), 1-48, 2014.
[27] P. Foti, M.R. Ayatollahi, F. Berto, Rapid strain energy density evaluation for V-notches under mode I loading conditions, *Engineering Failure Analysis*, **110**, 104361, 2020.
[28] P. Foti, S.M.J. Razavi, M.R. Ayatollahi, L. Marsavina, F. Berto, On the application of the volume free strain energy density method to blunt V-notches under mixed mode condition, *Engineering Structures*, **230**, 111716, 2021.
[29] Dassault. ABAQUS v. 6.14 User's Manual, Dassault Systemes.
[30] N. Gimsing, C. Georgakis, Cable Supported Bridges – Concept and Design – 3rd Edition, 2012. John Wiley & Sons.
[31] ERDC. Corrosion Induced Loss of Capacity of Post-Tensioned Seven Wire Strands Cable Used in Multistrand Anchor Systems Installed at Corps Projects, 2016 [Technical Report].
[32] Z. Jie, L. Susmel, High‐strength steel wires containing corrosion pits: stress analysis and critical distance based fatigue life estimation. *Fatigue & Fracture of Engineering Materials and Structures*, **43**, 1611–1629, 2020.